Compositional inhomogeneities in AlGaN thin films grown by molecular beam epitaxy: Effect on MSM UV photodetectors

Pallabi Pramanik, Sayantani Sen, Chirantan Singha, Abhra Shankar Roy, Alakananda Das, Susanta Sen, and A. Bhattacharyya'

Citation: J. Appl. Phys. **120**, 144502 (2016); doi: 10.1063/1.4964420
View online: http://dx.doi.org/10.1063/1.4964420
View Table of Contents: http://aip.scitation.org/toc/jap/120/14
Published by the American Institute of Physics

Compositional inhomogeneities in AlGaN thin films grown by molecular beam epitaxy: Effect on MSM UV photodetectors

Pallabi Pramanik,[1] Sayantani Sen,[1] Chirantan Singha,[1] Abhra Shankar Roy,[1] Alakananda Das,[2] Susanta Sen,[2] and A. Bhattacharyya[2,a)]
[1]*Centre for Research in Nanoscience and Nanotechnology, University of Calcutta, Kolkata 700106, India*
[2]*Institute of Radio Physics and Electronics, University of Calcutta, Kolkata 700009, India*

(Received 14 June 2016; accepted 25 September 2016; published online 11 October 2016)

Ultraviolet (UV) MSM photodetectors (PD) based on AlGaN alloys find many applications, including flame sensing. In this work we investigate the dependence of AlGaN based photodetectors grown by MBE on the kinetics of growth. MSM photodetectors were fabricated in the interdigitated configuration with Ni/Au contacts having 400 μm finger length and 10 μm finger spacing. Bulk $Al_{0.4}Ga_{0.6}N$ films were grown on to sapphire substrates using an AlN buffer layer. A series of PDs were developed using the $Al_{0.4}Ga_{0.6}N$ films grown under different group III/V flux ratios ranging from stoichiometric conditions to much higher than unity. Upon testing, it was observed that the otherwise identical photodetectors show significant decrease in dark current as AlGaN deposition conditions change from stoichiometric to excess group III, due to reduction of unintentional incorporation of oxygen-related point defects. In addition, the intensity and spectral dependence of the photocurrent also change, showing an extended low energy tail for the former and a sharp and prominent excitonic peak for the latter. The optical transmission measurements indicate a variation in Urbach energy with deposition conditions of the AlGaN films, although they have the same absorption edge. While all samples show a single red-shifted photoluminescence peak at room temperature, upon cooling, multiple higher energy peaks appear in the photoluminescence (PL) spectra, indicating that the alloys contain complex compositional inhomogeneities. Two types of alloy fluctuations, determined by the growth conditions, have been identified that modulate the optoelectronic properties of AlGaN by changing the spatial localization of excitons, thereby altering their stability. We identified that growth under stoichiometric conditions leads to compositional inhomogeneities that play a detrimental role in the operation of MSM photodetectors, which reduces the sharpness of the sensitivity edge, while growth under excess metal conditions enhances it. *Published by AIP Publishing*. [http://dx.doi.org/10.1063/1.4964420]

I. INTRODUCTION

AlGaN alloys have been studied extensively over the last two decades and have become the material of choice today for a range of semiconductor devices, from high speed transistors to ultraviolet optical emitters and detectors. These materials have been grown by the molecular beam epitaxy (MBE) as well as the metalorganic chemical vapor deposition (MOCVD) route, and devices such as UV light emitting diodes (LEDs) have been grown successfully by both these techniques. However, the external quantum efficiencies of such devices are significantly lower than those based on InGaN alloys and also show a large spread[1] depending on the number of parameters. The most critical of them is the presence of large dislocation densities due to the non-availability of native substrates, and the various point defects associated with them that act as non-radiative recombination centers. Different methods have been employed to increase radiative efficiency, including the lateral epitaxial overgrowth (LEO) process that significantly reduces dislocation densities. An alternative route is to promote the generation of compositional inhomogeneities by carefully controlling the surface diffusion length of adatoms during growth. This leads to spatial potential fluctuations, and the carriers diffuse to the localized potential minima and recombine from there, thus making the process relatively insensitive to the presence of crystal defects. Milliwatt power UV LEDs have been produced by both these techniques.[2,3] Another important application for AlGaN alloys has been in the field of UV detection, specifically in the solar-blind regime. Various devices have been reported, including photoconductive detectors,[4] planar and vertical Schottky photodiodes,[5] MSM devices in the interdigitated configuration,[6] PIN photodiodes[7] and avalanche photodiodes (APD),[8] with a range of sensitivities, gain and UV-to-visible rejection ratios. The effect of long range atomic order has been extensively studied in AlGaN photoconductive detectors[9] and mobility-lifetime product of such devices has been seen to increase significantly due to these effects. However, while systematic studies on the effect of compositional inhomogeneities have been carried out for UV LEDs,[3,10] similar studies on the optical properties of UV photodetectors are relatively rare.

In this paper, we investigate a wide range of surface kinetics of growth for AlGaN alloys by plasma assisted molecular beam epitaxy, while maintaining the alloy composition at a constant value of ~40% AlN mole fraction. The resultant variation in unintentional incorporation of oxygen-related point

a)Author to whom correspondence should be addressed. Electronic mail: anirban1@gmail.com

defects and localized compositional inhomogeneities as well as their effect on the optoelectronic properties of MSM photodiodes has been studied.

II. EXPERIMENTAL DETAILS

A. Growth and characterization of AlGaN films

The growth of AlGaN bulk films was carried out on 2-in. c-plane sapphire substrates using a VEECO Gen 930 MBE system using an RF Plasma source for nitrogen activation. Prior to growth, the substrates were outgassed at ~400 °C at a vacuum level of $\sim 10^{-9}$ T. A three step process was employed: (i) nitridation, (ii) buffer layer deposition and (iii) deposition of the active layer. Initially, the sapphire (Al_2O_3) substrate, maintained at 800 °C, was exposed to nitrogen plasma (450 W) to convert the top few layers to AlN. The nitridation process was terminated upon observation of a RHEED pattern corresponding to AlN.

Nitridation was followed by the deposition of an AlN buffer layer that was carried out at a substrate temperature of 800 °C and a reduced plasma power of 350 W. In this work, the AlN buffer layer was grown using a modified migration enhanced epitaxy process.[11,12] Initially, the growth was carried out under an excess group III flux using an Al beam equivalent pressure (BEP) of $\sim 1.9 \times 10^{-7}$ T for a short period of time ($t_{ON} \sim 10$ s), followed by an exposure to the nitrogen plasma. This process was repeated for the entire duration of the AlN growth with progressively longer durations of t_{ON}. At the end of the growth of the buffer layer, the RHEED pattern showed clear 2 × 2 reconstructions and a streaky nature. The thickness of the AlN buffer layer, as estimated from the growth rate, was about 65 nm.

The bulk AlGaN film was grown with a plasma power of 350 W and an Al BEP of 4.15×10^{-8} T at a substrate temperature ~800 °C. Gallium has a high desorption rate under these conditions, while Al has nearly 100% sticking coefficient. The group III/V flux ratio, which is determined by the arrival rates of aluminum, gallium and the active nitrogen species, as well as the desorption rate of gallium, can therefore be varied widely by very small changes in substrate temperature.[13] We identify three distinct growth regimes based on the III/V flux ratio: (a) excess group III conditions, where a metallic layer on the growth surface is formed that causes the RHEED pattern to become dim and diffuse due to scattering of the electron beam; (b) stoichiometric conditions, where the RHEED pattern is bright and streaky during growth; and (c) intermediate conditions. The thickness of the metallic layer differentiates the conditions (a) and (c). The difference can be directly observed by the variation of the RHEED pattern after closing the group III shutters.[14] The dim and diffuse RHEED pattern observed during growth (for $t_{ON} \sim 10$ min), when the group-III shutter is kept open, is recovered after the group III flux is shut off for a certain time (t_{OFF}) ranging from around 10 s to 30 s, resulting in a high-contrast pattern with clear surface reconstructions. This time duration t_{OFF} for a fixed t_{ON} is a direct measure of the thickness of the metallic layer on the growth surface and hence that of the III/V flux ratio employed.

We have investigated the optical properties of bulk AlGaN films grown under various III/V flux ratios—as given by the variation of the time taken for the RHEED pattern to change from a diffuse to a high-contrast state—and the corresponding optoelectronic properties of MSM photodetectors fabricated on such films. X-ray diffraction measurements were carried out on the as-grown AlGaN film, and the Al alloy composition was found to be 40%. Optical transmission measurements were carried out on bulk AlGaN films over 200 nm–600 nm range using a dual (30 W De/30 W QTH) lamp, a 0.5 m monochromator and a PMT detector. Photoluminescence (PL) measurements were carried out using the same setup and a quasi-CW 10 mW He-Ag laser with an emission at 224 nm as the excitation source. Low temperature measurements were carried out by mounting the sample on a 4 K close-cycle cryostat (Cryo Industries of America). Cathodoluminescence measurements have been carried out using a GATAN MONOCL4 system mounted on to a JSM 7600 F scanning electron microscope, using an acceleration voltage of 15 KV.

B. Fabrication and testing of interdigitated devices

Inter-digitated photodetector structures were fabricated on AlGaN films employing image reversal photolithography processes and lift-off technique using a Suss Microtec MA6/BA6 mask aligner and AZ5214E photoresist. A Ni/Au metallic stack (4 nm/13 nm) was used as the contact without any further annealing. A representative MSM device, along with its dimensions, is shown in Figure 1(b). Each device contains 23 fingers of length ~400 μm and width 10 μm and has a spacing of 10 μm between the adjacent fingers. Additional pads of Ni/Au (20 nm/60 nm) were deposited in a subsequent process, with a width of 100 μm to allow direct probing at the wafer level. A cross sectional schematic of a typical bulk AlGaN sample and the fabricated device is presented in Figure 1(a).

The devices were tested using a custom built probe station capable of carrying out spectroscopic measurements of the photodetectors at the wafer level. A Keithley 236 Source Measure Unit was used to perform the current-voltage measurements. A 30 W Deuterium lamp dispersed by a 0.25 m monochromator (Acton SP 2300 from Princeton Instruments) was used as the excitation source.

III. RESULTS AND DISCUSSION

A. Photodetector I–V characteristics

A series of MSM photodetectors were developed using identical conditions, except for the group III to group V flux ratio employed during AlGaN growth. The dark current-voltage characteristics measured for these devices are presented in Figure 2(a). Stoichiometric conditions were maintained for device D14, and the group III flux was progressively increased till it was significantly higher than unity for D1.

We can see a number of significant differences in the device characteristics as the conditions of AlGaN deposition are modified. For samples grown under excess group III, very

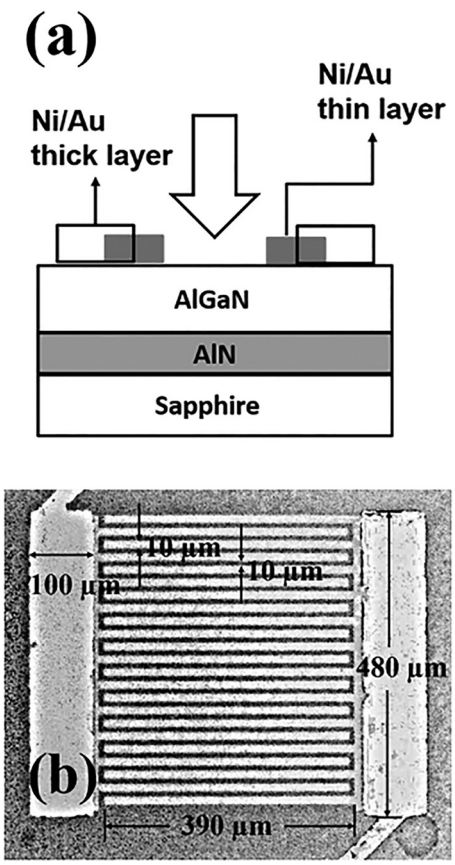

FIG. 1. Schematic (a) and photograph of interdigitated Ni/Au MSM photodetector device (b).

little current flows through the device under low bias conditions (~5 V), which increases by an order of magnitude as the bias is increased to 20 V. As the group III to group V flux ratio progressively reduces to stoichiometric conditions, the current at 5 V increases from 10^{-10} A to 10^{-6} A. However, the current at 20 V for the same samples increases from 10^{-9} A to $\sim 10^{-3}$ A, which is a very dramatic change, considering that the contacts are identical and no dopants have been deliberately added to the AlGaN material.

These current values at 20 V, measured under dark conditions, are again reproduced in Figure 2(b) and are compared with the excess current measured upon illumination of the sample with a deuterium lamp (henceforth referred to as the *photocurrent*). An aperture was employed to keep the intensity of the lamp deliberately low in order to reduce secondary effects. It can be observed that the photocurrent recorded also depends strongly on the group III to group V flux ratio employed during growth. This has been linked with the time required for the RHEED pattern to transition from a diffuse low contrast state to a high contrast state; when after growth is carried out under group III rich conditions for a time t_{ON}, the metal shutters are closed till the excess metal on the growth surface is incorporated into the film (t_{OFF}). The ratio of this "clearing time", t_{OFF} to t_{ON}, has been included for various samples in Figure 2(b) and ranges from 0.1 for high group III rich conditions to zero for stoichiometric samples. For samples grown under excess group III (D1, D2, D3, D4, and D5), the photocurrent, like the dark current, is low but is significantly higher (as much as 20 times) than the dark current. As the samples are grown closer to stoichiometric conditions, both dark current and photocurrent increase very significantly. However, as stoichiometric condition is approached, the dark current reaches a value significantly large compared to the photocurrent. The dark and photocurrent measurements on each individual device were carried out without altering the probe setup to minimize the effect of measurement uncertainty. Therefore, the effects are due to material related issues, rather than variations in the measurement conditions.

The variation in dark current is linked with the change in the resistivity of bulk AlGaN film, as the sapphire substrate and the AlN buffer layers are insulating. As stated before, no deliberate doping was carried out, so the samples are doped by background impurities during growth or by point defects. It should be noted that the growth was carried out in an MBE system with background vacuum better than 10^{-10} T, using 6.5N nitrogen passed through Gate Keeper® inline purifiers before injecting into the RF plasma source. Still, oxygen is typically present in trace amounts in MBE systems, usually adsorbed or bonded to metallic contaminants on the chamber walls. Oxygen is a traditional n-type dopant in III-nitride materials and is expected to have higher affinity for AlGaN than for GaN films.[15] Nitrogen vacancies are the other possible n-type defects. But in the present context, since the dark current, which is a measure of

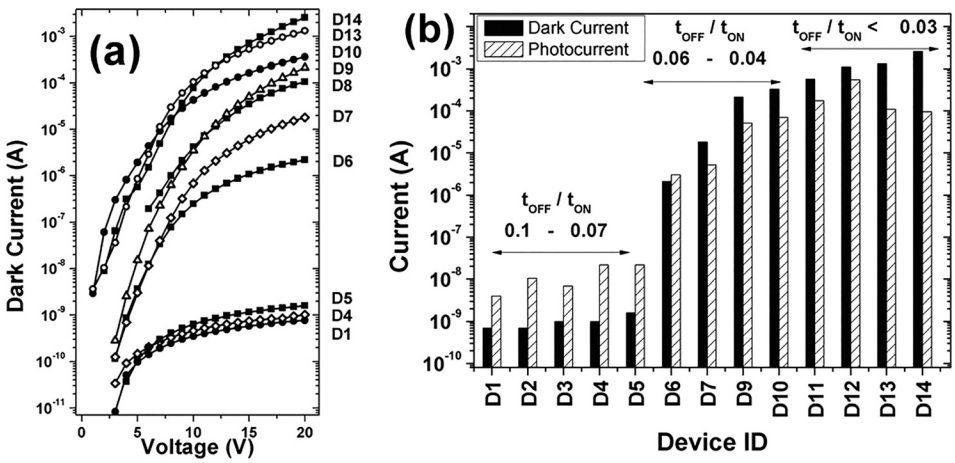

FIG. 2. I–V characteristics (a) and variation of dark/photocurrent (b) for various Ni/Au MSM photodetectors (see text).

background carrier concentration, sharply decreases with increased group III to group V ratio, nitrogen vacancies can be ruled out. The incorporation of ambient oxygen into GaN film has been shown previously to be strongly dependent on the group III to group V ratio employed.[16–18] The metallic gallium film present on the surface during growth under group III-rich conditions bonds with the ambient oxygen, forming volatile gallium oxide that subsequently desorbs at the growth temperature, and hence their incorporation into the film underneath is limited. This phenomenon cannot take place for the stoichiometric films, as the presence of excess Ga that can arrest the oxygen is limited, and hence the films are doped n-type by the incorporated oxygen.

We believe that these phenomena are present in the current study, magnified by the increased affinity of Al to Oxygen. This can be clearly observed in Figure 2, where for samples grown with excess group III, small changes of group III to V ratio—as long as the metallic coverage is present during growth—do not make a significant difference (sample D1–sample D5). Reducing the group III further causes a large change in the dark current.

An increase in photocurrent with an increased oxygen doping can be easily explained from the large dislocation densities present in these films. The threading dislocations generate dangling bonds at each atomic layer it passes through, which act as traps for free carriers generated by optical excitation. Thus, the low levels of optical excitation for undoped AlGaN films produce little photocurrent. However, when oxygen doping is present, these traps are compensated and the excess carriers generated by optical excitation produce a strong photocurrent. Therefore, with growth conditions approaching stoichiometry, both the dark and the photocurrent can be observed to strongly increase.

The fact that the dark current increases with voltage at a much faster rate for stoichiometric samples, however, cannot be explained without taking into account the variation of the barrier height at the metal-semiconductor junction, which in turn is related to the change in electron affinity, as the metal work-function remains the same. This suggests that there is a change in the band-alignment, at least at the local level, with the variation of the growth kinetics.

B. Photocurrent spectra

The effect of the growth kinetics on the photodetector properties was also investigated by determining the spectral dependence of the photocurrent, and the results are presented in Figure 3. The spectra are normalized and are vertically separated for easy comparison.

As noted before, samples D1–D5, grown under excess group III conditions where a metallic layer was present during growth, showed very low dark current values but a strong increase in photocurrent upon UV excitation. It can be seen in Figure 3 that these detectors show a sharp Gaussian peak at ~290 nm, which is due to excitonic transitions. For shorter wavelengths, the photocurrent maintains a high and relatively steady value, while a sharp cutoff with little band-tailing is present at longer wavelengths.

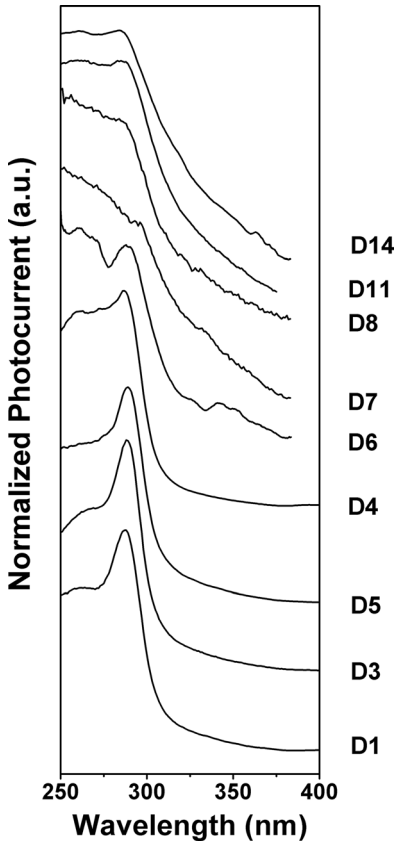

FIG. 3. Photocurrent spectrum obtained from various MSM photodetectors.

The nature of the photocurrent spectrum changes with a reduction in group III to V flux ratio. The excitonic peak disappears and is replaced by a transition edge that becomes progressively less steep. Significant band-tailing can be seen for near-stoichiometric conditions, but for these samples a weak excitonic peak reappears, as can be observed for samples D11 and D14.

Excitonic peaks have been routinely reported in the GaN photodetectors and are generated by an increased sensitivity—that is an increase in absorption coefficient—at corresponding energies. It should be noted that the exciton must be split by the applied field in order to contribute to the photocurrent. Figure 3 indicates that the formation of excitons and their binding energies are strongly dependent on the group III to group V flux ratio, i.e. on the kinetics of growth. We postulate that these effects are linked with the spatial localization of carriers that determine the formation and subsequent splitting of excitons under an applied bias. In order to establish the link between photodetector characteristics and the carrier localization processes, a number of optical characterization steps were carried out on the bulk AlGaN film, as presented in Sec. III C.

C. Optical characterization of AlGaN alloys

1. Absorption spectra

The invariance of the sensitivity edge for various photodetectors in Figure 3 indicates that the average alloy composition remains identical despite the change in growth kinetics. This is further validated by the optical transmission measurements

carried out for the AlGaN films, as shown in Figure 4. From the nearly identical nature of the transmission spectra, it can be inferred that the optical absorption edge is the same for all the samples. This has been established by determining the peak of the derivative of the absorption coefficient with respect to energy, which identifies the absorption edge, as shown in the inset in Figure 4. For higher energies, the absorption coefficient is dependent on the $E^{1/2}$ nature of the density of states function, while for lower energies, it is given by the Urbach tail, which is a measure of the binding energy of excitons.[19,20] The measurement indicates that the absorption edge remains the same within an experimental error for the three representative group of samples. Furthermore, the presence of prominent optical interference fringes in the transmission band indicates a smooth surface morphology for all the samples.

Upon close examination, however, we see that below the absorption edge there is a systematic variation of the slope of the absorption spectra with a variation in the growth conditions, as shown in Figure 5(a). The slope of the absorption edge has been usually linked with the Urbach tail, which dominates at energies slightly lower than the band-gap. The absorption coefficient (α) at photon energies below the optical band gap exponentially depends on the photon energy (E) by the following relation:

$$\propto (E) = e^{\frac{E-E_g}{E_u}}, \quad (1)$$

where E_g is the band gap of the semiconductor and E_u is known as the Urbach energy. The Urbach energy of the samples was calculated from the slope of the absorption coefficient and is presented in Figure 5(b) for samples grown with different III/V flux ratios. It shows that the Urbach energy increases from ~115 meV to 180 meV as the flux ratio used during growth changes from sample D1 (excess group III) to sample D11 (stoichiometric). Comparing this result with Figure 3, we observe that the increased Urbach energy is reflected in the enhanced band-tailing for the photodetectors.

The Urbach energy is a measure of the disorder of the system, which can be either structural or due to compositional inhomogeneities. For AlGaN alloys, the alloy disorder dominates, as reported by Bajaj *et al.*,[21] increasing with AlN mole fraction till about 70% and then subsequently decreasing sharply. This was determined by the width of the photoluminescence excitonic peak.

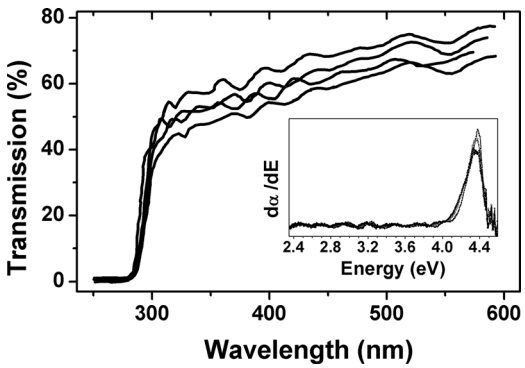

FIG. 4. Optical transmission spectra for AlGaN bulk films.

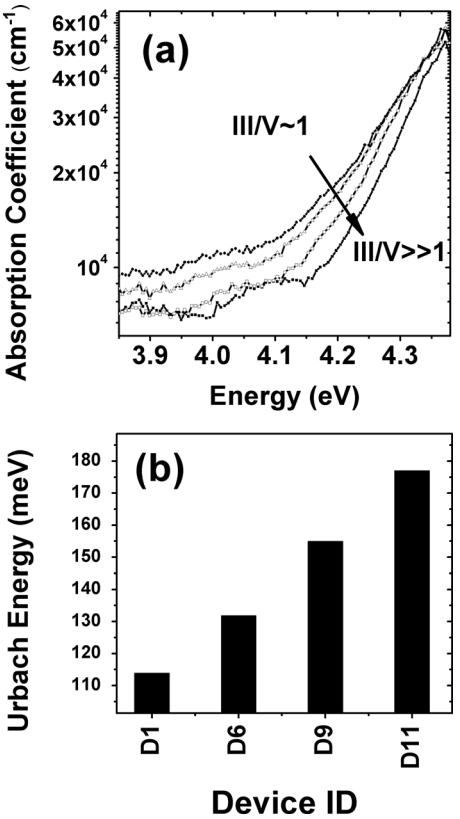

FIG. 5. Absorption spectrum of AlGaN bulk films (a) and Urbach energy of AlGaN bulk films (b).

2. Photoluminescence spectra

Photoluminescence spectra are another measure of disorder in these alloys, and such measurements have been carried out on the samples described previously. They were measured at room temperature (RT) for samples grown under different group III/V flux conditions and are presented in Figure 6. A single peak is observed in all the cases. Also, the CL spectrum (shown in the inset) measured across wider wavelength ranges does not show any prominent sub-bandgap luminescence peak. This indicates that these materials are of good quality and do not contain deep impurities. This also eliminates the possibility that the disorder observed in the optical absorption studies is structural in nature.

Figure 6 indicates that the AlGaN films grown under near stoichiometric conditions show the strongest PL peak, centered at 315 nm, which is red-shifted by as much as 400 meV compared to the absorption edge. This red-shift correlates with the fact that the Urbach energy was the highest for this sample. While a red-shift is present for all the samples, it becomes less pronounced with increasing group III to group V flux ratio. There is also a significant narrowing of the PL peak with increasing III-to-V ratio. Interestingly, there is a small but clear asymmetry for all the peaks, with a slightly longer tail on the higher energy side. This is different from low-energy band-tails typically observed in III-Nitride films, which are attributed to various disorder effects. In order to understand this phenomenon, low temperature PL measurements were carried out for three selected representative

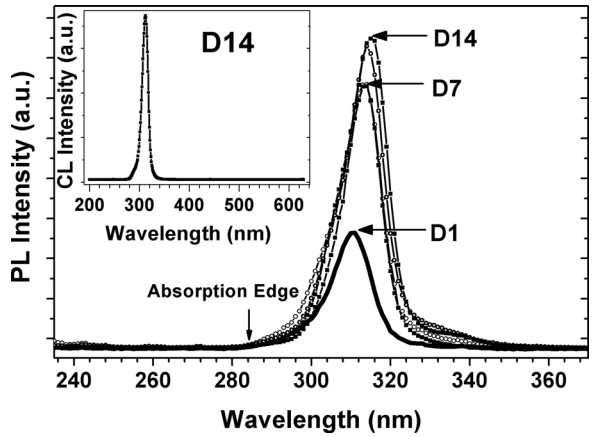

FIG. 6. Room temperature photoluminescence (RTPL) spectra for AlGaN samples grown under various group III/V flux ratios (the inset shows the cathodoluminescence spectra of the sample (D14) grown under stoichiometric regime).

samples grown under regimes ranging from very excess group III to stoichiometric.

In Figure 7, the temperature dependent PL spectra are given for AlGaN films corresponding to the samples D1 (III/V $\gg$ 1), D7 (III/V $>$ 1) and D14 (III/V $\sim$ 1). In the inset, the room temperature spectra are again provided for comparison.

For stoichiometric sample D14, the relatively broad PL peak observed at room temperature splits into two with cool-down, producing a sharper peak at 312 nm and a wider peak at 303 nm at 4 K (Figure 7(a)). The width of the sharper peak (peak C) reduces to 4 nm at 4 K. Furthermore, below 180 K, an additional peak (peak A) evolves at shorter wavelengths, becoming dominant at 4 K.

For AlGaN films grown under high excess group III, the RT peak does not split but progressively blue-shifts to 305 nm with a decrease in temperature (Figure 7(c)). Similar to the previously described sample, at a temperature below 200 K, an additional high energy peak emerges and this dominates at 4 K.

A clear distinction can be seen for samples grown under slightly excess group III. Instead of sharp and clear peaks, a broad luminescence can be seen that can be fitted to three Gaussian distributions.

The shift of the PL peak energy as a function of temperature for all three samples is presented in Figure 8, where the room temperature peak position is taken as the reference. For stoichiometric sample D14, each of the three peaks shows distinct temperature dependencies. The position of the peak at the longest wavelength (indicated by "C") remains mostly invariant with temperature, albeit showing a weak S-type behavior, where the peak position initially blue shifts with cool down, then red shifts and finally blue shifts again. The other two peaks show a steady blue-shift with cool-down. For samples grown under excess group III (D1), only two peaks were observed at low temperatures. In Figure 8, therefore, there are only two curves for this sample, as the lowest energy peak is absent. The two peaks clearly correspond with the peaks A and B from the previously described sample in their temperature dependence. For samples grown under slightly excess group III, as mentioned before, a broad luminescence

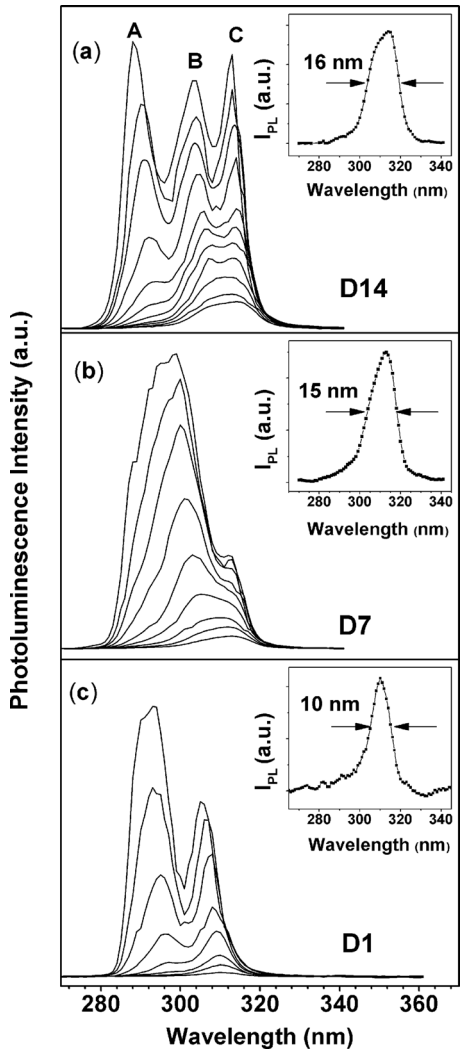

FIG. 7. Temperature dependent PL for (a) D14 (III/V $\sim$ 1), (b) D7 (III/V $>$ 1) and (c) D1 (III/V $\gg$ 1) (the inset of each figure shows the corresponding RTPL).

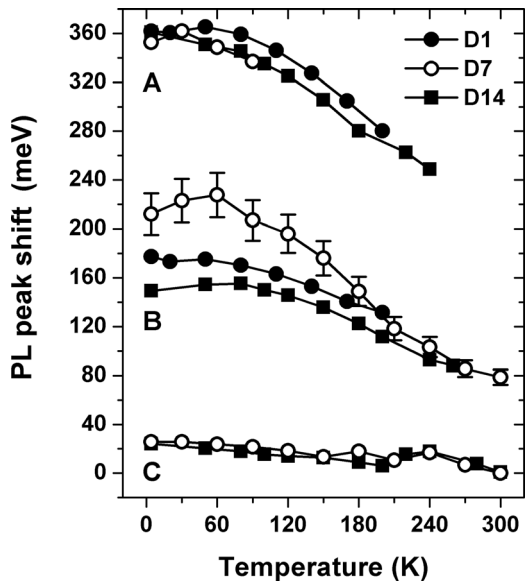

FIG. 8. Dependence of peak position shift on temperature for the peaks obtained from the temperature dependent PL spectra of samples D14(III/V $\sim$1), D7(III/V $>$ 1) and D1(III/V $\gg$ 1).

is observed instead of clear peaks at all temperatures, which could be fitted to three Gaussian distributions. The three calculated peak positions obtained from these Gaussian fits are plotted in Figure 8 for this sample. In spite of large error bars due to fitting inaccuracies, it can be observed that all three peaks A, B, and C are represented in this sample, but they are significantly broader, leading to the overlap.

We believe that the highest energy peak (peak A), which appears only at low temperatures and has the highest intensity for all three samples, corresponds with the photoluminescence from band-to-band recombination. This happens because at low temperatures the thermal energy of the carrier is low enough to restrict them from diffusing significantly, and hence they recombine primarily from their points of generation. The other peaks observed at higher temperatures occur due to the transport of the photo-excited carriers to localized potential minima that are caused by compositional inhomogeneities in the material and subsequent excitonic recombination from such locations. Multiple long wavelength PL peaks indicate the presence of compositional inhomogeneities with different nature and amplitudes in the same AlGaN film, as shown in Figure 9. At room temperature, the carrier transport being maximum, most of them can move to the lowest potential minima and recombine from there. This leads to a larger red-shift of the room temperature PL peak with respect to the absorption edge and a corresponding increase in its intensity.

D. Summary of results

Alloy fluctuations in AlGaN alloys have been reported by several groups, and these effects are more prominent for MBE grown films, as they are grown under the kinetic, rather than thermodynamic regime. In the absence of spinodal decomposition, these fluctuations have been linked to a number of alloy phenomena, including a long range atomic ordering. This ordering can be of monolayer type,[22] of complex type, or may be completely incommensurate,[23] depending on the alloy composition, that is, the AlN mole fraction, as well as the group III to group V flux ratio employed during growth. The complex and incommensurate ordering however have been reported[22] only for high AlN mole fraction (70%–87%) and were absent for lower values such as those employed in this work.

The study of monolayer (1 × 1) ordering has been carried out by a number of groups for samples grown by PA-MBE.[24,25] Their results indicate that for ordered structures, AlGaN alloys can be seen as spontaneously formed superlattices where the carriers are localized in the GaN layer. The optical band-gap may red-shift by as much as 100 meV with respect to the disordered structures formed by annealing of the samples. In addition, studies on ordering in AlGaN alloys have demonstrated that the bowing parameter strongly depends on the degree of ordering. The observed reduction of the band gap with ordering was also supported by Dudiy and Zunger[16] using first principle calculations. The complexity increases due to the presence of ordered and disordered domains that are present side-by-side within the same material under certain growth conditions. These domains have been shown to form a type II heterostructure that significantly affects the recombination properties.[15] Iliopoulos *et al.* however demonstrated that the monolayer ordering in AlGaN alloys is more prevalent when the growth takes place under N-rich conditions[22] and therefore is not relevant to this work, where excess group III conditions are employed.

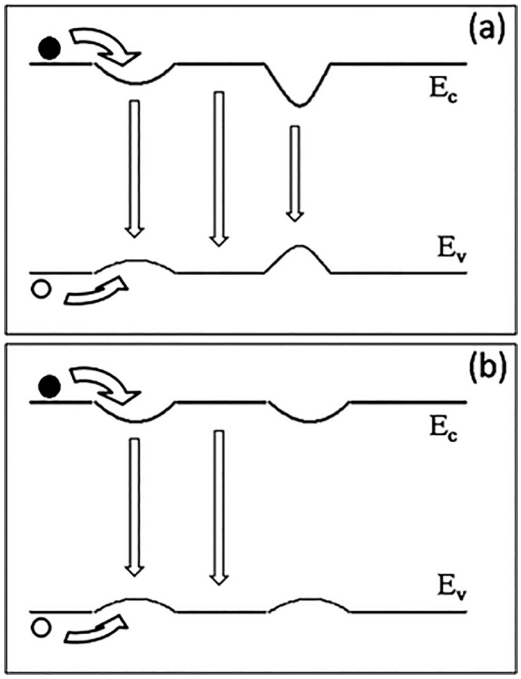

FIG. 9. Model of potential fluctuation produced in samples grown under different group III/V flux ratio regimes (a) stoichiometric and (b) excess group III.

Local in-plane compositional inhomogeneities have also been reported by several groups: e.g., Gao *et al.* have demonstrated phase segregation in AlGaN alloys.[26] They have also concluded that the phase segregation has a strong dependence on the relative diffusion lengths of Al and Ga on the growth surface. They demonstrate that a small variation of 20°–30° C temperature across the growth surface plays a very significant role in controlling the nature and magnitude of the alloy modulation amplitude. This effect has also been observed by Collins *et al.*,[27] who reported that compositional inhomogeneities can be generated by limiting the surface mobility of the Al adatom by appropriate choice of growth parameters.[27] This is applicable in the current study for the samples grown under stoichiometric conditions. For the samples grown under high group III conditions, the excess metal stabilizes at the growth surface with some statistical thickness and compositional variation. The AlGaN film is formed with the reaction of active nitrogen with this metallic layer, and thus these variations are replicated in the short-range lateral fluctuation of the composition of the AlGaN alloys. While the average alloy composition remains invariant for all the samples studied in this work, the localized fluctuations in composition affect the carrier localization properties in UV MSM photodetectors. The generation of photocurrent in III-nitride films involves the generation of electron-hole pairs, which can then form excitons, which subsequently need to be split by the applied electric field. The formation

probability and stability of the excitons are higher when the carriers are spatially localized at potential minima such as those generated by compositional fluctuations. Our results indicate that it is the nature of fluctuations that determine the optoelectronic properties of AlGaN based photodetectors.

The low temperature photoluminescence spectra show that the strongest fluctuations occur for stoichiometric films, which at all temperatures is dominated by a peak at ~310 nm, which is significantly red shifted from the band-edge. This peak becomes progressively less prominent, as the group III is increased and is absent for growth under excess metal conditions. We relate the presence of this peak with the strong band-tailing effects that is observed in both the optical transmission and the photocurrent spectra. This type of compositional inhomogeneity appears to be detrimental to the performance of UV MSM photodetectors, drastically reducing selectivity and rejection ratio. Under excess group III, the absorption edge is much sharper and a prominent and sharp excitonic peak is observed, indicating that the compositional fluctuations generated due to the presence of a metallic film present on the growth surface are less detrimental for the operation of photodetector. This is supported by a larger photocurrent to the dark current ratio observed for these samples under the same bias conditions.

IV. CONCLUSIONS

MSM photodetectors have been fabricated from AlGaN alloys grown under different growth conditions, where the spatial inhomogeneity of the alloy at the localized scale has been controlled by varying the group III to group V flux ratio. Our results indicate that this variation makes very significant changes to the values of both the dark current and the photocurrent. In addition, the spectral dependence of the photodetector is also modified, with sharp exciton-related peaks observed under group III-rich conditions and long band-tails observed for stoichiometric conditions.

We identified two different pathways through which the group III to group V ratio may affect the optoelectronic properties of MSM photodiodes. Under excess group III conditions, the presence of metallic gallium on the growth surface prohibits the incorporation of oxygen—which is an n-type dopant—in the AlGaN film by forming volatile gallium oxide; a phenomenon that is absent for AlGaN films grown under stoichiometric conditions. This oxygen incorporation causes a very strong variation of the magnitude of the dark and photocurrents in these devices grown under a range of group III to group V flux ratios.

Additionally, the variation of growth mode leads to the generation of two different types of compositional inhomogeneities in the AlGaN film. One type occurs under stoichiometric conditions due to limited mobility of Al adatom. The other occurs under group III rich conditions, where the surface is coated with a metallic layer, the compositional fluctuations of which are reflected in the AlGaN film deposited by its interaction with active nitrogen. Our results indicate that the first type of compositional inhomogeneity adversely affects the wavelength selectivity and rejection ratio of MSM photodetectors by generating long absorption tails and increased values of Urbach energy, while the second type improves the device performance, leading to a sharp sensitivity edge and a narrow excitonic peak.

For the development of focal-plane-array-based UV imagers on a commercial scale, where larger wafer sizes are likely to be employed, small variations of substrate temperature and hence gallium desorption rate are challenging to avoid. This will inevitably lead to variations in the group III to V ratio across the wafer. Our results indicate that this must be avoided due to a very prominent influence of the group III to group V ratio and hence growth kinetics on sensitivity as well as the spectral properties of ultraviolet photodetectors. The use of a surfactant such as Indium during the growth of AlGaN alloys at high substrate temperature may mitigate these effects to a large extent.[28]

ACKNOWLEDGMENTS

This work was partially funded by the Department of Information Technology (12(3)/2011-PDD), Government of India. P.P., S.S., and A.D. would like to acknowledge the Council of Scientific and Industrial Research Senior Research Fellowship (CSIR-SRF) scheme, and C.S. would like to acknowledge the Department of Science and Technology (DST) INSPIRE fellowship for funding their work.

[1]M. Kneissl, T. Kolbe, C. Chua, V. Kueller, N. Lobo, J. Stellmach, A. Knauer, H. Rodriguez, S. Einfeldt, Z. Yang, N. M. Johnson, and M. Weyers, Semicond. Sci. Technol. **26**, 014036 (2011).
[2]J. P. Zhang, A. Chitnis, V. Adivarahan, S. Wu, V. Mandavilli, R. Pachipulusu, M. Shatalov, G. Simin, J. W. Yang, and M. A. Khan, Appl. Phys. Lett. **81**, 4910 (2002).
[3]Y. Liao, C. Thomidis, C. Kao, and T. D. Moustakas, Appl. Phys. Lett. **98**, 081110 (2011).
[4]B. W. Lim, Q. C. Chen, J. Y. Yang, and M. A. Khan, Appl. Phys. Lett. **68**, 3761 (1996).
[5]N. Biyikli, I. Kimukin, T. Kartaloglu, O. Aytur, and E. Ozbay, Phys. Status Solidi C **0**, 2314 (2003).
[6]M. Gokkavas, S. Butun, T. Tut, N. Biyikli, and E. Ozbay, Photonics Nanostruct. Fundam. Appl. **5**, 53 (2007).
[7]M. B. Reine, A. Hairston, P. Lamarre, K. K. Wong, S. P. Tobin, A. K. Sood, C. Cooke, M. Pophristic, S. Guo, B. Peres, R. Singh, C. R. Eddy, Jr., U. Chowdhury, M. M. Wong, R. D. Dupuis, T. Li, and S. P. DenBaars, Proc. SPIE **6119**, 611901 (2006).
[8]R. McClintock, A. Yasan, K. Minder, P. Kung, and M. Razeghi, Appl. Phys. Lett. **87**, 241123 (2005).
[9]M. Misra, D. Korakakis, H. M. Ng, and T. D. Moustakas, Appl. Phys. Lett. **74**, 2203 (1999).
[10]A. V. Sampath, G. A. Garrett, R. W. Enck, P. Rotella, Jr., H. Shen, and M. Wraback, Phys. Status Solidi C **8**, 1534 (2011).
[11]G. Namkoong, E. Trybus, K. K. Lee, M. Moseley, W. A. Doolittle, and D. C. Look, Appl. Phys. Lett. **93**, 172112 (2008).
[12]T. D. Moustakas and A. Bhattacharyya, Phys. Status Solidi C **9**, 580 (2012).
[13]E. Iliopoulos and T. D. Moustakas, Appl. Phys. Lett. **81**, 295 (2002).
[14]M. Moseley, D. Billingsley, W. Henderson, E. Trybus, and W. A. Doolittle, J. Appl. Phys. **106**, 014905 (2009).
[15]T. D. Moustakas and M. Misra, Proc. SPIE **6766**, 67660C (2007).
[16]S. V. Dudiy and A. Zunger, Appl. Phys. Lett. **84**, 1874 (2004).
[17]M. L. Nakarmi, N. Nepal, J. Y. Lin, and H. X. Jiang, Appl. Phys. Lett. **86**, 261902 (2005).
[18]T. D. Moustakas and A. Bhattacharyya, ECS Trans. **35**(6), 63–71 (2011).
[19]C. H. Qiu, C. Hoggatt, W. Melton, M. W. Leksono, and J. I. Pankove, Appl. Phys. Lett. **66**, 2712 (1995).
[20]S. Chichibu, T. Mizutani, T. Shioda, H. Nakanishi, T. Deguchi, T. Azuhata, T. Sota, and S. Nakamura, Appl. Phys. Lett. **70**, 3440 (1997).

[21]G. Coli, K. K. Bajaj, J. Li, J. Y. Lin, and H. X. Jiang, Appl. Phys. Lett. **80**, 2907 (2002).
[22]E. Iliopoulos, K. F. Ludwig, Jr., T. D. Moustakas, and S. N. G. Chu, Appl. Phys. Lett. **78**, 463 (2001).
[23]Y. Wang, A. S. Özcan, K. F. Ludwig, Jr., A. Bhattacharyya, T. D. Moustakas, L. Zhou, and D. J. Smith, Appl. Phys. Lett. **88**, 181915 (2006).
[24]M. Albrecht, L. Lymperakis, J. Neugebauer, J. E. Northrup, L. Kirste, M. Leroux, I. Grzegory, S. Porowski, and H. P. Strunk, Phys. Rev. B **71**, 035314 (2005).
[25]M. Benamara, L. Kirste, M. Albrecht, K. W. Benz, and H. P. Strunk, Appl. Phys. Lett. **82**, 547 (2003).
[26]M. Gao, S. T. Bradley, Yu Cao, D. Jena, Y. Lin, S. A. Ringel, J. Hwang, W. J. Schaff, and L. J. Brillson, J. Appl. Phys. **100**, 103512 (2006).
[27]C. J. Collins, A. V. Sampath, G. A. Garrett, W. L. Sarney, H. Shen, M. Wraback, A. Yu. Nikiforov, G. S. Cargill III, and V. Dierolf, Appl. Phys. Lett. **86**, 031916 (2005).
[28]P. Pramanik, S. Sen, C. Singha, A. S. Roy, A. Das, S. Sen, A. Bhattacharyya, D. Kumar, and D. V. S. Rao, J. Cryst. Growth **439**, 60–65 (2016).